Applied Biochemistry and Biotechnology (2022) 194:4081–4092
https://doi.org/10.1007/s12010-022-03977-7

ORIGINAL ARTICLE

Restoration of the Indicator Properties of Whole-cell Luminescent Biosensors

D. B. Kuznetsov[1,2] · A. Yu. Mironov[2] · V. A. Neschislyaev[1] · I. L. Volkhin[3] · E. V. Orlova[1] · A. D. Shilina[1]

Accepted: 16 May 2022 / Published online: 25 May 2022

Abstract
Whole-cell biosensors are widely used to produce medical diagnostic tests, but in the long term, they tend to lose their indicator properties. Consequently, it is crucial to find ways to restore these properties and prolong the shelf life of the tests. Here, we propose to use electromagnetic radiation with optimally selected parameters of frequency, power, and exposure time. The impact of radiation parameters on biosensor luminescence was studied as well as the effects of different types of radiation coming from laser sources (λ = 875 nm), a LED source (λ = 850 ÷ 890 nm), and microwave units (at frequencies 42.22, 53.53, 61.18 и 34 ÷ 38 GHz). IR treatment resulted in dose-dependent suppression of biosensor luminescence. The luminescence level when exposed to microwave radiation depends on the radiation time and frequency. Also, it has been found that optimal selection of the main radiation parameters enables to restore indicator properties partially lost by biosensors during storage. We explain the mechanism responsible for the sensitizing effect of radiation, which implies the polarization of solvent dipoles and changes in mobility of acceptor molecules. This, in turn, leads to a shift in the chemical equilibrium states and triggers a cascade of biochemical reactions that lead to restoration of the lost indicator properties of biosensors. The study of antagonistic activity has revealed that restored biosensors provide reliable test results after the expiration of their warranty period.

Keywords Bioluminescence · Biosensor · Luciferase · Electromagnetic radiation

Introduction

Modern analytical research based on the application of different biosensors provides rapid and highly reliable results [1, 2]. There are whole-cell biosensors (WCB) represented mainly by transgenic organisms which, due to their luciferase expression,

✉ D. B. Kuznetsov
denis.pfa@gmail.com

1 Perm State Pharmaceutical Academy, Perm 614000, Russian Federation

2 G. N. Gabrichevsky Moscow Research Institute for Epidemiology and Microbiology, Moscow 125212, Russian Federation

3 Perm State University, 614000 Perm, Russian Federation

generate a bioluminescent analytical signal [3]. Bioluminescence provides good spatial resolution and allows for a simple quantitative evaluation of the signal [4, 5]. Being originally designed for use in biomedicine, environmental and agricultural monitoring, WCBs are sensitive to environmental factors and able to respond to many types of impacts [6].

The most sensitive, efficient, and time-proven method of analysis is the analysis using an optical WCB [7]. There are fluorescent, bioluminescent, and colorimetric WCBs. The most common WCB is a fluorescent one, which is based on green fluorescent protein (GFP). Fluorescent WCBs are so popular because of the stability of a molecule, the sensitivity, and simplicity of the construction. Yet, this type of a biosensor has a significant disadvantage. During analysis, these biosensors must be labeled with fluorescent reagents, which increases the time and cost of the procedure [7]. Bioluminescent WCBs, however, do not have this drawback and allow efficient detection of even very low concentrations of substances [8]. One of such biosensors is WCB "Ecolum-8", based on E. coli with a lux-operon. This WCB has proven to be a reliable tool for determining the integral action of various compounds of different nature (hydrocarbons, heavy metals, phenols, pesticides, etc.) as well as for determining the impact of electromagnetic radiation (EMR) on bacterial cells [9–11]. The change in the bioluminescence level of the test strain under the influence of EMR is due to changes in the functioning of the electronic transport chain whose work is connected with the generation of light quanta, as well as with the participation of active oxygen forms in these processes [11].

Whole-cell biosensors have substantial benefits including obtaining results in the shortest possible time, not having to transport samples, reduced labor intensity of sample preparation and analysis, no need for highly qualified laboratory specialists, the possibility of on-site investigation without use of expensive equipment. All these factors significantly reduce the cost of the research [12].

The above suggests that WCBs are expected to rapidly evolve into more automated, compact, and wireless devices for real-time detection of a variety of environmentally significant pollutants [13].

Despite their obvious potential, WCBs have several limitations. One of these is the fact the growth phase of cells affects the noise in the system and makes reproducibility difficult. Besides, some compounds cannot penetrate through the cell membrane and, therefore, sensing mechanisms are unable to detect them. In addition, many contaminants remain toxic to the host organism [14]. Furthermore, one of the main problems is that during storage, even under optimal conditions, the indicator properties decrease, affecting the test results and the shelf life [7]. Thus, it is essential to find ways to restore the properties of the WCB indicator, which is the main goal of the given research.

To date, as already mentioned, no methods are reported to be able to restore the properties of the WCB indicator. In our previous papers, we showed that microwave radiation can influence biomass growth and the level of *E. coli luminescence* [15, 16]. Such treatment of WCBs is supposed to be able to restore WCB indicator properties. However, information on the non-thermal non-resonant effect of microwave radiation on WCB is extremely limited. This study is the first to show the possibility of restoring the indicator properties of a biosensor, which can extend its shelf life. We also describe the main stages of the mechanism that affects biosensors. In the future, this will allow the development of new microwave radiation methods and the design of devices for their implementation, which will produce various useful effects.

Materials and Methods

Object of Research

The research used WCB Ecolum-8 based on *E. coli* K12 TG1 hsd R17 hsdM thi relAl sup E44 Δ (lac-pro AB) F' (traD36 proAB + lac lq lacZΔM15 with a *lux*-operon *Photoharbdus luminescens* ZM1) [17] and production strain *E coli* LEGM-18 obtained at the Institute of Ecology and Genetics of Microorganisms of the Ural Branch of the Russian Academy of Sciences and deposited in the All-Russian Collection of Industrial Microorganisms of the FSUE State Research Institute of Genetics. Cultivation was carried out under standard conditions at + 37 °C.

The above strain was used to study the effect of EMR on the integral toxicity of wastewater of different levels of contamination [18]. The authors of this study recommend the use of WCBs for the rapid detection of biological effects.

Research of Bioluminescence

Preparation of samples for bioluminescence research included rehydration of the lyophilized indicator test strain of bacteria with 0.9% solution of sodium chloride cooled to 6 ± 2 °C, and preparation of working dilution with purified water with pH 7.0 ± 0.2 and cooled to a temperature of 6 ± 2 °C. After 30 min of exposure to a temperature of (6 ± 2) °C the diluted suspension of the indicator strain was removed from the refrigerator and left at 22 ± 2 °C for at least 30 min. The test culture was poured into 1 ml polymer tubes and placed in the experimental unit for EMR treatment. The luminescence level of the experimental and control samples of the biosensor was determined at 22 ± 2 °C and pH $6.5 \div 8.0$. The operation of "Biotox-10" (LLC HEPA-S, Russia) was carried out according to the operating manual.

To study the effect of EMR on the biosensor parameters of "Ecolum-8", we carried out experiments involving express-tests. The effect of radiation treatment was expressed as luminescence index values in imp/sec or as a luminescence index (dimensionless value): luminescence index $K = \frac{I1-I2}{I1}$ where I_1 and I_2 are the luminescence intensity of the indicator strain without irradiation and after it, respectively [19]. The increase of glow rate is directly proportional to the inhibitory effect, and the decrease is directly proportional to the stimulating effect.

Experimental Setups

The experiments were carried out within the infrared and microwave ranges of electromagnetic waves using three experimental setups. Figure 1a shows a schematic of the device for irradiation of samples within the infrared (IR) wave range. The device used was MILTA-F-8–01. A solid-state injection laser [1] with a pulse radiation power of 21 W at wavelength $\lambda = 875$ nm served as the coherent radiation. The duration of laser radiation pulses was 70 ns, pulse repetition rate was 5 kHz. Four LEDs [2] with a total power of 100 mW generated radiation in the range of $\lambda = 850 \div 890$ nm. The body of the device [3] was covered from above with a reflective aluminum plate [4]. The tube

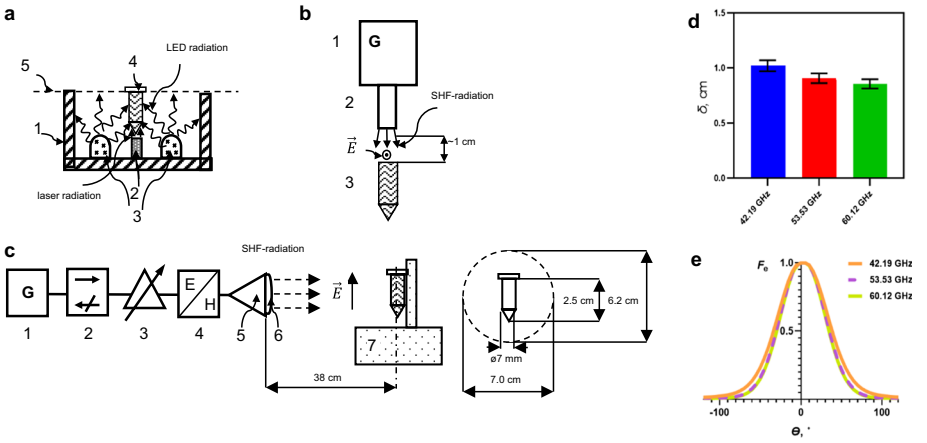

Fig. 1 Schematic of the setup for sample irradiation and conditions for EMR treatment (**a**) SHF-radiation λ = 7.1, 5.6 и 4.9 mm; (**b**) Irradiation λ = 850 ÷ 890 nm; (**c**) SHF-radiation at frequencies 34 ÷ 38 GHz; (**d**) Skin-layer δ cm of nutrient medium GRM-broth; (**e**) DP in Cartesian coordinate system with relative scale

containing the sample [5] was inserted into the central hole so that from below it was irradiated by the laser and by LEDs from the sides.

For work within a super-high-frequency-radiation range (SHF) two experimental setups were used. A schematic of the setup which worked at fixed SHF frequencies of 42.22, 53.53, 61.18 GHz is shown in Fig. 1b. Microwave generator MILTA-CHF with an output power of 10 mW was equipped with a circular cross-section antenna [2]. A divergent beam of microwave radiation at a distance of 1 cm from the antenna aperture had a half-power cross-section, like a circle with a radius of 3.5 mm. A test tube with an internal diameter of 7 mm containing the culture under study was placed coaxially to the axis of the SHF-radiation beam.

Figure 1c shows a schematic of the setup used for the research within the SHF range of 34–38 GHz. The antenna-wave path consisted of a generator G4-156 (1), ferrite isolator (2), attenuator (3), matching transformer (4), horn antenna (5), and a lens (6). A detailed description of the setup is given in [15]. The tube containing the sample (7) was irradiated with 0.4 mW/cm^2 microwave radiation flux. Projection of the test tube onto a microwave beam of half-power cross-section is presented on the right side of the figure. The variation in sample temperature during the experiment was less than 1 °C.

Search for Optimal Conditions for EMR Treatment

When treating a WCB by EMR, the fact should be taken into account that water is the main component of living organisms and any change in its properties such as molecular alignment, protons transportation, and the aqueous environment of polymers can be of great importance. During EMR treatment, part of the energy is stored while the other part is consumed. The density of the stored energy is proportional to the dielectric permeability of the substance while the consumed energy is proportional to the absorption coefficient. In nonmagnetic liquids, absorption is related to dielectric losses [20, 21]. Concerning the absorption spectrum of liquid water, there is strong absorption of radiation in the range of millimeter radiation [22]. Special attention should be paid to the indices of dielectric

permeability and dielectric medium losses within this range. There is a probability that to obtain a biological effect, the dielectric permeability of the medium and the dielectric loss should be relatively equal [23].

EMR treatment can be carried out, provided that the intensity is reduced by no more than 2.71 times. Numerous studies have tried to identify the conditions under which all cells of microorganisms are found in the EMR field of approximately similar intensity. For this purpose, the thickness of the skin layer in the medium, the boundary of the far zone, and the antenna direction pattern were determined.

To calculate the absorption capacity of the medium, we studied electrical resistance R_m. Measurements were taken for 3.5 min. It was found that the medium FHM-broth (harvest broth for microorganism cultivation, dried fishmeal hydrolysate) has an electrical resistance of $R = 532 \pm 53$ Ohm.

Calculation of the Skin Layer in FHM-Broth

To determine the depth of microwave penetration into the FHM-broth medium, we used experimental data of electrical resistance and the parameters of electromagnetic radiation generators applied. Specific electrical conductivity $\sigma_m = \left(\frac{c}{abR}\right) = 0.058 \pm 0.009$ Ohm^{-1} m^{-1}, where, $a = 18$ mm, $b = 29$ mm, $c = 16$ mm — liquid layer dimensions, R — electrical resistance. The thickness of the skin layer $\delta = \sqrt{\frac{2}{2\pi f \mu_m \mu_0 \sigma_m}}$, where f is the frequency of microwave radiation, μ_m — relative magnetic permeability of the medium ($\mu_m = 1$), μ_0 — magnetic permeability of vacuum ($4\pi \times 10^{-7}$ H/m). The results for each mode are shown in Fig. 1d.

Far Zone Boundary

The far zone of the antenna is the area in which radiation flow density is inversely proportional to the area of the distance from the antenna. Directional properties of the antenna (directional diagram) in the far zone depend only on the angular direction, unlike the Fresnel zone where the directional properties are determined by the laws of geometric optics. The far zone was calculated by the formula $R \geq \frac{2D^2}{\lambda}$ where R is the far zone radius, D is the antenna aperture diameter, λ is the wavelength (GOST R 51,317.4.3–99) (Table 1).

Directional Diagram

The open end of a circular waveguide served as a radiating antenna. A directional diagram (DD) for this type of radiator has one main lobe and several side lobes. Most of the

Table 1 Radiation characteristics depending on the generator mode

Mode	Wavelength λ, mm	Frequency f, GHz	Antenna aperture diameter D, mm	Radiation intensity, mW/cm^2	Far-zone radius R, mm	Half-power cross-sectional diameter $D_{1/2}$, mm
1	7.1	42.19	5.0	2.0	7.0	18
2	5.6	53.53	4.5	2.5	7.2	16
3	4.9	60.12	4.0	2.8	6.5	15

radiation energy is concentrated in the main lobe which is almost symmetrical. Typically, the antenna concentrates most of the energy in one direction. Therefore, we calculated the unit-normalized DD only for the main lobe using the formula: $F_{\mathrm{e}} = \frac{P(\theta)}{P_{max}} = \frac{\lambda_0^2}{4\pi^2 D^2} \frac{\sin^2\left(\frac{\pi D}{\lambda_0}\sin\theta\right)}{\sin^2\theta}(1+\cos\theta)^2$ where F_e — DP value in the direction of the antenna radiation, $P(\theta)$ — angular radiation power, P_{max} — maximum power, θ — angular direction, D — diameter of the open end of the waveguide, λ_0 — free-space wavelength. Normalized to unity, the directional diagram is represented in Fig. 1e.

Diameter $D_{1/2}$ of the cross-section of the half power microwave beam at 1 cm from the antenna was calculated (Table 1).

Based on the calculations of DP and skin layer, the following conditions for the experiment were proposed: the distance from the resonator output to the phase interface should be ≥ 10 mm; the diameter of the container must not exceed the width of the main lobe. Providing these conditions are met, all cells of microorganisms are found in the half-power field of electromagnetic radiation.

Results and Discussion

The choice of WCB on *E. coli* basis for the study is caused by several factors that influence the efficiency of these biosensors and the quality of luminescent testing. Such factors include stability of the test culture and reproducibility of bioluminescence analysis results.

If the sample strain is stored for a long time, its indicator properties may degrade, which will affect the test results. Thus, maintaining the indicator properties of the biosensor is an essential task, including the use of EMR potential.

To study the influence of EMR on the improvement of the indicator properties of the *E. coli* strain, the procedure was divided into two stages: (1) The study of the influence of different types of EMR treatment on the luminescence of the Ecolum-8 biosensor and the selection of optimal modes. (2) Comparative study of the luminescence level of the irradiated and unirradiated test strain after 24 h of cultivation with the addition of unirradiated *E. coli* LEGM-18 culture.

At the first stage, we studied the luminescence characteristics of a biosensor under the influence of infrared and microwave radiation. The data on the changes in the biosensor luminescence response over time exposed to IR radiation with different durations, which was obtained during this stage, showed its versatile nature (Fig. 2a). The increase in the duration of radiation from 2 to 10 min led to a transition from stimulation of glow to its suppression. Two- and 5-min IR treatment did not lead to a significant change in the luminescence level. IR treatment for 10 min led to a considerable decrease in luminescence intensity, which after an hour recovered to a control sample value (0). Among the modes of operation of the test system exposed to IR, the necessary mode to solve the problem was not found. The study of the luminescence under microwave radiation showed a difference in the luminescence reaction compared to that obtained under IR treatment. Millimeter microwave treatment for 1 h immediately caused luminescence of the biosensor. Such treatment ensured luminescence stimulation throughout the whole experiment (Fig. 2).

An important aspect of using microwave radiation to treat the test culture strains is the fact that their indicator properties are not distorted. Therefore, the next step was to carry out comparative tests of the indicator properties of the irradiated and unirradiated test strain cultures in a co-incubation with a potential production strain of *E. coli*

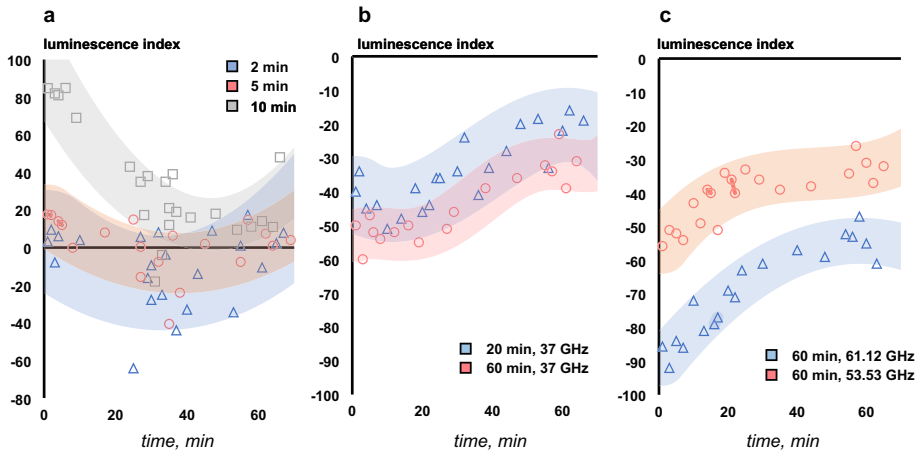

Fig. 2 Change of biosensor luminescence level after EMR treatment. Value «0»—control (sample without radiation). The sign (-) indicates an increase in luminescence compared to the control. (**a**) IR treatment $\lambda = 850 \div 890$ nm. (**b**) and (**c**) SHF-radiation treatment

Table 2 Luminescence levels of irradiated and unirradiated biosensor when adding *E. coli* LEGM-18 culture

	Control value	Without radiation		After radiation	
Exposure time (min)	Luminescence level, cps	Luminescence level, cps	Change compared to control (%)	Luminescence level, cps	change compared to control (%)
30 min	5309 ± 1275	4498 ± 1679	− 15.3 ($P = 0.027$)	5597 ± 940	5.4 ($P = 0.37$)
60 min	5223 ± 939	4095 ± 1124	− 21.6 ($P = 0.04$)	5241 ± 1188	0.4 ($P = 0.65$)
90 min	5001 ± 933	4128 ± 1112	− 17.4 ($P = 0.03$)	5409 ± 1464	8.2 ($P = 0.75$)

The sign (−) indicates a decrease compared to control values.

LEGM-18 (Table 2). The evaluation of the indicator properties of the test strain was carried out by measuring its luminescence level after 30, 60, and 90 min. It has been found that after long-term storage the luminescence of the samples was between 15.27% and 21.6% lower than that of control values. Nevertheless, after low-intensity microwave radiation, the luminescence level recovered to its control value. Comparative analysis of changes in the luminescence index revealed no statistically significant difference ($p > 0.05$) between irradiated samples and control samples of sensor system Ecolum-8. Thus, the exposure of a biosensor to SHF-radiation to improve the test system's stability has proved to be promising and does not lead to data distortion in bioluminescent testing. This effect may have practical value when restoring indicator properties of a biosensor after long storage, which will ensure the extension of the shelf life of system Ecolum-8 and, accordingly, improve its consumer properties.

Because SHF radiation is strongly absorbed by water, it is possible that it can influence the migration of protons in the water and lead to their redistribution in the "environment-cell" system. These phenomena were described in detail in [15].

The results of the luminescence test of the biosensor after exposure to EMR showed different patterns of the luminescence reaction. To explain the possible mechanism of influence of EMR on the biosensor, we consider known bioluminescence mechanisms.

The first mechanism is a modified version of chemically initiated electron exchange luminescence. According to this mechanism, the oxidative potential of flavine probably affects the bioluminescence reaction rate, which was observed in experiments with analogs of the substituted flavine mononucleotide (FMN) [24]. In the first step, FMN undergoes a double bond rearrangement, which results in the transfer of one electron from FMN to dioxygen and the transfer of a proton from an unidentified base to a dioxygen molecule. Then, the FMN and dioxygen radical molecules enter into a binding reaction to form FMN-peroxo-adducts. The carbonyl carbon of the aldehyde substrate deprotonates the peroxide product, which by nucleophilic addition attacks the carbonyl carbon of the aldehyde substrate. FMN gives one electron to the peroxo-group, causing homolysis of the O–O bond. His44 deprotonates the intermediate, causing homolysis of the C-H bond, with one electron transferred to the oxygen radical and the other to the carbon of the broken C-H bond. Bound oxygen in FMN deprotonates His44. Negatively charged oxygen in the intermediate product initiates the transfer of one electron from the intermediate product to FMN, which then emits a photon. The hydroxyl group bound to FMN initiates the removal of intramolecular water to form an FMN product [25, 26].

The second mechanism is based on the Baeyer–Villiger mechanism, according to which FMN-peroxo-adduct after its formation can nucleophilically attack an aldehyde substrate to form an intermediate product. Upon collapse, this product transfers hydride to the second oxygen of the peroxo-adduct, which results in the cleavage of the peroxide bond.

This makes the intermediate C (4a)-hydroxyflavine excited, making it emit a blue-green light when it returns to the ground state. The hydroxyl bound to FMN initiates intramolecular water removal and its release, as well as production of FMN [25, 26].

The third mechanism, like the previous ones, follows a reaction in which, after rearrangement of the FMNH2 double bond and production of a radical by the addition of oxygen to the flavine, an intermediate capable of nucleophilic interaction with the aldehyde substrate is formed. The resulting flavine C (4a)-peroxyhemiacetal decomposes to form intermediate dioxyran and intermediate C (4a)-hydroxyflavin in their excited states, which then decompose to their ground state and emit a blue-green light. The intermediate product undergoes intramolecular removal, causing the release of water and the formation of the final FMN product [25–27].

In all the three mechanisms, water molecules serve as proton donors. In addition, those unidentified bases are probably the dissociation products of water molecules in these reactions. This, in turn, can explain how radiation, which is supposed to be absorbed by water molecules, can affect the intensity of biosensor luminescence and the duration of the effect. The mechanism of the impact of EMR on biosensor bioluminescence is shown below (Fig. 3).

Two mechanisms can be used to explain this phenomenon; the first one is based on the concepts of colloidal chemistry, and the second one is based on the concepts of surface chemistry. The first mechanism involves the description of the observed phenomenon according to the theory of "long-range chemotaxis" which occurs due to the gradients of concentration of ions OH^- or H^+ [28, 29]. The process of EMR absorption causes changes in the concentration gradients of these ions due to the presence of a stock of exchangeable H^+ ions in polymers that can exchange with cations in the solution and create an inhomogeneous distribution of ions (salt gradient) in a liquid [30].

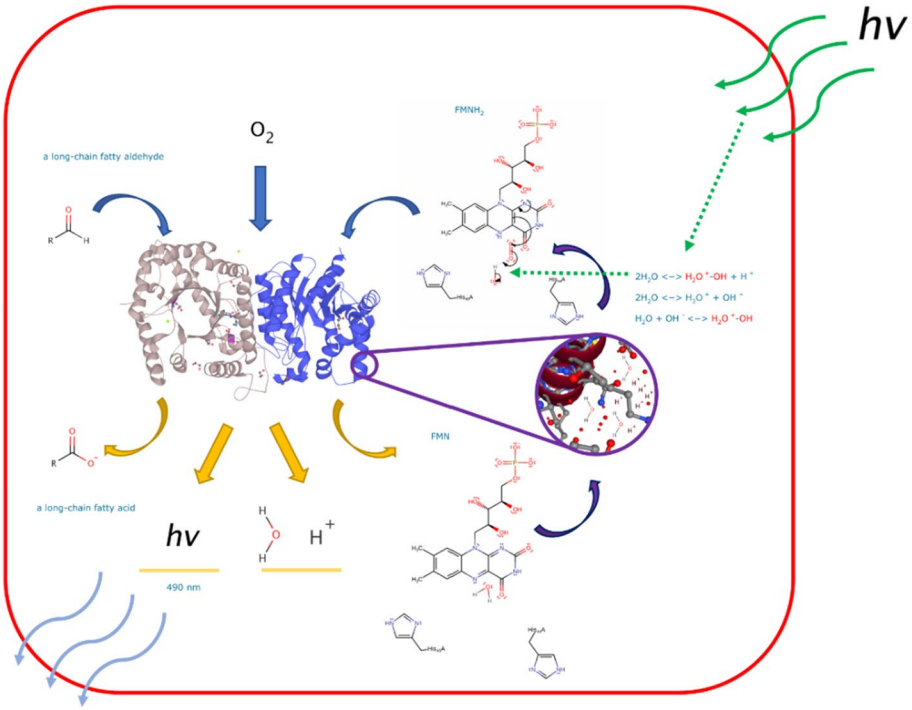

Fig. 3 Effect of EMR on luminescence of biosensor Ecolum-8

The second mechanism is related to the effect of EMR on the thickness of the adsorbed water phase [15, 16]. The main aspect about understanding the formation of the adsorbed phase under the influence of EMR is that the more radiation energy is absorbed by the system, the thicker the adsorbed phase. Unlike other wavelengths, millimeter radiation and infrared EMR are known to be strongly absorbed by water molecules, and less so by proteins and nucleic acids. Notably, proteins of secondary structure, mostly α-helices and β-sheets, can serve as a surface for epitaxy from the liquid phase. Thus, the process of changing the properties of a biosensor affects the whole life activity of the cell and cannot be considered a local process occurring in the near-surface luciferase. The described mechanism may be only a small fragment of the overall mechanism of microwave exposure, as the description of the whole process would be extremely complicated.

The effects of EMR on biosensor luminescence can be explained by the structure of a bacterial luciferase molecule consisting mainly of α-spirals and a pocket. The structure of luciferase contains adsorption centers for water molecules (Fig. 3). The active center is located within a large inner cavity of the α-subunit (shown in purple) [31].

Treatment by EMR of certain wavelengths is aimed at shifting the water dissociation equilibrium, at changing the processes of ion transfer in the near-surface spaces, as well as at densification and expansion of the adsorbed phase due to redistribution of the electron density in acceptor-molecules. A dissociation shift of the water equilibrium is accompanied by cascade reactions of charge separation with the accumulation of H^+ ions outside the adsorbed phase [32–34]. H^+ ions are known to exist in a liquid medium

in the form of various proton complexes: H_3O^+, $H_3O_2^-$, $H_5O_2^+$, which can play the role of ligands, including bridging ones [35, 36].

Under the action of quanta of an electromagnetic field on α-helices of proteins, including those of luciferase, the epitaxial growth of the adsorbed phase is initiated (Fig. 3). Driven out ions H^+ increase their concentration gradient $\Delta\mu H^+$ in acid reservoirs. The energy of absorbed radiation is converted into the energy of the dipole–dipole interaction and is accumulated in the layers of adsorbed water and in the gradient $\Delta\mu H^+$ [15]. Displaced protons reduce FMN (flavinmonucleotide) to $FMNH_2$. The excess energy is carried away from a living system through a series of reactions and is released as quanta of light radiation $h\nu 2$ (37). This study considers only local processes of the effects of ENR on WSBs. However, it should be taken into account that this will affect host cells. Proton concentration gradient $\Delta\mu H^+$ is the major energy source for any cell, and, accordingly, its change can lead to a change in the physiological status of the entire living system as our previous studies showed [15, 16].

The proposed mechanism allows us to explain how EMR, which is generally absorbed by water molecules, can have a long-lasting effect on the luminescent response of the sensory system. Nevertheless, this assumption requires further verification. The data presented in the study expand the understanding of the effects of microwave radiation on WCB and its practical value. The proposed method of restoring the indicator properties can be considered a simple solution to the problem of WCB stability.

Conclusions

The type of radiation associated with microwave treatment has been chosen and the parameters have been determined which allow increasing the luminescence level of a biosensor and restoring its indicator properties after long-term storage. In the course of comparative studies of indicator properties, it has been found that the difference in the development of luminescence response of the experimental and control samples to similar antagonistic action is insignificant. This study confirms that EMR treatment of WCBs does not cause any distortion of their indicator properties. That is why the use of EMR for the restoration (correction) of biosensor indicator properties can be considered a promising method.

The research is the first to show the possibility of restoring the properties of a biosensor indicator, which allows for the extension of its shelf life. The research also provides an explanation of how EMR affects biosensors. In the future, this may allow the development of new microwave radiation methods and devices for their implementation, bringing various benefits.

Author Contribution D.B. Kuznetsov: Conceptualization, Methodology, Data curation, Formal analysis, Project administration, Writing original draft, Visualization. A.Yu. Mironov and V.A. Neschislyaev: Conceptualization, Data curation, Methodology, Formal analysis, Writing—review & editing. I.L. Volkhin: Writing—Review & Editing, Formal Analysis. E.V. Orlova: Formal analysis, Supervision, Project administration. A.D. Shilina: Validation, Data curation, Visualization.

Declarations

Consent for Publication All authors give their consent to the publication.

References

1. Moraskie, M. et al. (2021). Microbial whole-cell biosensors: Current applications, challenges, and future perspectives. Biosensors & Bioelectronics 113359-113376 https://doi.org/10.1016/j.bios.2021.113359
2. Berepiki, A., Kent, R., Machado, L. F., & Dixon, N. (2020). Development of high-performance whole cell biosensors aided by statistical modeling. *ACS Synthetic Biology., 9*(3), 576–589. https://doi.org/10.1021/acssynbio.9b00448
3. Cai, S., et al. (2018). Engineering highly sensitive whole-cell mercury biosensors based on positive feedback loops from quorum-sensing systems. *The Analyst, 143*(3), 630–634. https://doi.org/10.1039/C7AN00587C
4. Kotlobay, A. A., Kaskova, Z. M., & Yampolsky, I. V. (2020). The palette of Luciferases Natural biotools for new applications in biomedicine. *Acta Naturae, 12*(2), 15–27. https://doi.org/10.32607/actanaturae.10967
5. Moraskie, M. et al. (2021). Microbial whole-cell biosensors: Current applications, challenges, and future perspectives. Biosensors & Bioelectronics 113359 https://doi.org/10.1016/j.bios.2021.113359
6. Fahliyani, S.A., Rastegari, A.A., Yadav, A.N., & Yadav, N. (2020), In new and future developments in microbial biotechnology and bioengineering: Microbially derived biosensors for diagnosis, monitoring, and epidemiology for future biomedicine systems (Rastegari A.A.,ed), Elsevier, pp. 43–65. https://doi.org/10.1016/B978-0-12-820528-0.00005-3
7. Dai, C., & Choi, S. (2013). Technology and applications of microbial biosensor. *OJAB., 2*, 83–93. https://doi.org/10.4236/ojab.2013.23011
8. Khudyakova, A. V., et al. (2019). Estimation of the toxicity of a metal/carbon nanocomposite of copper by biotesting. *Bulletin of the Russian Academy of Sciences, 46*(10), 1359–1363. https://doi.org/10.1134/S1062359019100145
9. Maksimova, A. V., Kuznetsova, M. V., & Demakov, V. A. (2016). The impact of synthetic nitriles on the morphology and viability of some bacterial species. *Bulletin of the Russian Academy of Sciences, 43*(6), 547–553.
10. Zarubina, A. P., Gapochka, M. G., Novoselova, L. A., & Gapochka, L. D. (2013). Effect of low-intensity electromagnetic radiation on the toxicity of domestic wastewater tested with the "Ecolum" test system. *Moscow Univ. Biol. Sci. Bull., 68*(1), 49–52. https://doi.org/10.3103/S0096392512030108
11. Bahadır, E. B., & Mustafa, K. S. (2015). Applications of commercial biosensors in clinical, food, environmental, and biothreat/biowarfare analyses. *Analytical Biochemistry, 478*, 107–120. https://doi.org/10.1016/j.ab.2015.03.011
12. Bilal, M., & Iqbal, H. M. (2019). Microbial-derived biosensors for monitoring environmental contaminants: Recent advances and future outlook. *Process Safety and Environment Protection, 124*, 8–17. https://doi.org/10.1016/j.psep.2019.01.032
13. Chang, H. J., Voyvodic, P. L., Zúñiga, A., & Bonnet, J. (2017). Microbially derived biosensors for diagnosis, monitoring, and epidemiology. *Microbial Biotechnology, 10*(5), 1031–1035. https://doi.org/10.1111/1751-7915.12791
14. Kuznetsov, D. B., et al. (2017). Epitaxy of the bound water phase on hydrophilic surfaces of biopolymers as a key mechanism of microwave radiation effects on living objects. *Colloids and Surfaces B, 154*, 40–47. https://doi.org/10.1016/j.colsurfb.2017.03.014
15. Kuznetsov, D. B., et al. (2019). Microwave radiation effects on the process of Escherichia coli cultivation. *Microbiology and Biotechnology Letters, 47*(3), 372–380. https://doi.org/10.4014/mbl.1810.10024
16. Danilov, V. S., Zarubina, A. P., & Eroshnikov, G. E. (2002). Sensory bioluminescent systems based on the lux-operons of different species of Luminescent Bacteria. *Vestn. Moscow un-that. Ser. Biology, 3*, 20–24.
17. Zarubina, A.P., Gapochka, M.G., Novoselova, L.A., & Gapochka, L.D. (2012). Biotesting of influence of the electromagnetic field of low intensity on the toxicity of the sewage water by the test system «Ecolum». Moscow Univ. Biol.Sci. Bull. 3, 43. 39–43. https://vestnik-bio-msu.elpub.ru/jour/article/view/63?locale=en_US
18. Neschislyaev, V. A., Pshenichnov, R. A., Archakova, E. G., Chistokhina, L. P., & Fadeeva, I. V. (2002). Method of assay of antagonistic activity of probiotics. *Patent of Russia, 2187801*(C2), 1–7.
19. Stenishchev, I. V., & Basharin, A. A. (2017). Toroidal response in all-dielectric metamaterials based on water. *Science and Reports, 7*(1), 1–9. https://doi.org/10.1038/s41598-017-07399-y
20. Bordonsky, G. S., Orlov, A. O., & Schegrina, K. A. (2017). Dielectric losses in supercooled pore water at a frequency of 34 GHz. *RAQE, 59*(10), 812–820. https://doi.org/10.1007/s11141-017-9750-x

21. Carlson, S., Brünig, F. N., Loche, P., Bonthuis, D. J., & Netz, R. R. (2020). Exploring the absorption spectrum of simulated water from MHz to the infrared. *Journal of Physical Chemistry A, 124*(27), 5599–5605. https://doi.org/10.1021/acs.jpca.0c04063
22. Andryieuski, A., Kuznetsova, S. M., Zhukovsky, S. V., Kivshar, Y. S., & Lavrinenko, A. V. (2015). Water: Promising opportunities for tunable all-dielectric electromagnetic metamaterials. *Science and Reports, 5*, 13535. https://doi.org/10.1038/srep13535
23. Hartmann, S., et al. (1999). NIH shift in flavin-dependent monooxygenation: Mechanistic studies with 2-aminobenzoyl-CoA monooxygenase/reductase. *PNAS, 96*(14), 7831–7836. https://doi.org/10.1073/pnas.96.14.7831
24. Romero, E., et al. (2018). Same substrate, many reactions: Oxygen activation in flavoenzymes. *Chemical Reviews, 118*(4), 1742–1769. https://doi.org/10.1021/acs.chemrev.7b00650
25. Tinikul, R., & Chaiyen, P. (2016). Structure, mechanism, and mutation of bacterial luciferase. Adv Biochem. *Eng. Biotechnol. Adv. Biochem. Eng. Biotechnol., 154*, 47–74. https://doi.org/10.1007/10_2014_281
26. Campbell, Z. T., Weichsel, A., Montfort, W. R., & Baldwin, T. O. (2009). Crystal structure of the bacterial luciferase/flavin complex provides insight into the function of the β subunit. *Biochemistry, 48*(26), 6085–6094. https://doi.org/10.1021/bi900003t
27. Schurr, J. M., Fujimoto, B. S., Huynh, L., & Chiu, D. T. (2013). A theory of macromolecular chemotaxis. *The Journal of Physical Chemistry B, 117*(25), 7626–7652. https://doi.org/10.1021/jp302587d
28 Schurr, J. M. (2013). Phenomena associated with gel–water interfaces. Analyses and alternatives to the long-range ordered water hypothesis. *The Journal of Physical Chemistry. B, 117*(25), 7653–7674. https://doi.org/10.1021/jp302589y
29. Elton, D. C., Spencer, P. D., Riches, J. D., & Williams, E. D. (2020). Exclusion zone phenomena in water—A critical review of experimental findings and theories. *International Journal of Molecular Sciences, 21*(14), 5041–5054. https://doi.org/10.3390/ijms21145041
30. Tinikul, R., Chunthaboon, P., Phonbuppha, J., & Paladkong, T. (2020). Bacterial luciferase: Molecular mechanisms and applications. *The Enzymes., 47*, 427–455. https://doi.org/10.1016/bs.enz.2020.06.001
31. Zheng, J. M., & Pollack, G. H. (2003). Long-range forces extending from polymer-gel surfaces. *Physical Review E, 68*(3), 031408–031414. https://doi.org/10.1103/PhysRevE.68.031408
32. Chai, B., Yoo, H., & Pollack, G. H. (2009). Effect of radiant energy on near-surface water. *The Journal of Physical Chemistry B, 113*(42), 13953–13958. https://doi.org/10.1021/jp908163w
33. Pollack, G. H. (2015). Cell electrical properties: Reconsidering the origin of the electrical potential. *Cell Biology International, 39*(3), 237–242. https://doi.org/10.1002/cbin.10382
34. Ogata, Y., Kawashima, Y., Takahashi, K., & Tachikawa, M. (2015). Theoretical vibrational spectra of OH−(H_2O)2: The effect of quantum distribution and vibrational coupling. *Physical Chemistry Chemical Physics: PCCP, 17*, 25505–25515. https://doi.org/10.1039/C5CP03632A
35. Gorlova, O. et al. (2016). Characterization of the primary hydration shell of the hydroxide ion with H2 tagging vibrational spectroscopy of the OH−·(H_2O) n= 2, 3 and OD−·(D_2O) n= 2, 3 clusters. The Journal of Physical Chemistry. 145(13), 134304–1–134304–8. https://doi.org/10.1063/1.4962912
36. Lee, J., Müller, F., & Visser, A. J. (2019). The sensitized bioluminescence mechanism of bacterial luciferase. *Photochemistry and Photobiology, 95*(3), 679–704. https://doi.org/10.1111/php.13063